International Communications in Heat and Mass Transfer 100 (2019) 35–41

Contents lists available at ScienceDirect

International Communications in Heat and Mass Transfer

journal homepage: www.elsevier.com/locate/ichmt

Comparative study on heat transfer enhancement by turbulent impinging jet under conditions of swirl, active excitations and passive excitations

Naseem Uddin[a,*], Bernhard Weigand[b], Bassam A. Younis[c]

[a] Mechanical Engineering Programme, Universiti Teknologi Brunei, Brunei Darussalam
[b] Institut für Thermodynamik der Luft- und Raumfahrt, Universität Stuttgart, Stuttgart, Germany
[c] Department of Civil and Environmental Engineering, University of California, Davis, USA

ARTICLE INFO

Keywords:
Turbulent impinging jet
Heat transfer enhancement
Passive and active excitations
Swirl

ABSTRACT

This paper reports on computations related to a turbulent jet impinging on a flat surface. The goal was to assess the efficiency of alternative methods for enhancing the heat-transfer rates at the target wall. Three methods were considered, all of which involved the manipulation of the jet flow at exit. These were the imposition of a tangential component of motion simulating the generation of swirl by guide vanes, the forced excitation of the mean flow at predetermined amplitude and frequency, and by the placement of a cylinder across the flow from which vortex shedding occurred. The computations were performed using Large-Eddy Simulations and the results compared with experimental data wherever available. It was found that the selection of active excitation frequency plays an important role in terms of enhancement of heat transfer. On the other hand, the passive excitation of the jet by introducing inserts in the flow causes high pressure drop while the introduction of swirl does not always bring about an appreciable enhancement in the heat transfer rates.

1. Introduction

It is well accepted that the heat transfer rates associated with the impingement of a jet on a target wall, a flow that has many engineering applications, can be increased through the imposition of swirl or of periodic excitations at the jet's inlet. The excitations may be introduced passively or actively. The jet's dynamics can be significantly altered and controlled through manipulation of different jet modes. The most amplified frequency in the jet, scaled with the initial momentum layer thickness and jet exit velocity, gives the shear-layer mode (Strouhal number scaled with most amplified frequency and shear-layer momentum thickness). Shear-layer mode plays significant role when the jet is issued from the orifice. However, in case of fully developed turbulent flow, the jet's preferred mode plays an important role [1] as excitations at this mode lead to significant changes in the jet's behaviour. Additionally, parameters like the jet's outlet-to-target wall distance, Reynolds number, amplitude of excitation, nozzle shape, and inlet velocity profile are also important when heat transfer enhancement is considered. Gau et al. [2] found that jet excitation plays an important role for short jet's outlet-to-target wall distances, especially when the nozzle-to-plate distance is < 4, and excitations are added at specific frequencies. Hwang and Cho [3] found that excitation promotes vortex pairing when the jet is excited at a subharmonic of the fundamental frequency. Sheriff and Zumbrunnen [4] found that the effect of pulsatile jet flow on heat transfer is only appreciable when the amplitude of pulsation is $< 40\%$ of the averaged inlet flow velocity. Beyond this amplitude, the heat transfer was found to decrease. Travnicek et al. [5] experimentally investigated the heat transfer enhancement or suppression by synthetic jets, a primary round jet and the complex case of a jet under helical and bifurcating modes by using flow visualization, hot-wire anemometry, PIV, and the Naphthalene sublimation technique. They found that for a small nozzle-to-wall spacing (e.g. $H/D = 2$) excitations led to a heat transfer increase in the stagnation area only. The jet's excitations has also been investigated numerically using DNS by Jiang et al. [6], and using LES by Uddin et al. [7].Fewer researchers investigated passive jet excitation. Herwig et al. [8] investigated the effects of unsteadiness on impinging jet heat transfer. The unsteadiness was introduced through a circular ring triggering periodic vortex shedding in the flow, precessing effect and alternating flow passages. They found that the heat transfer can be augmented only for the Karman jet nozzle in which additional unsteadiness and turbulence is introduced without fundamentally changing the flow structure of the jet. Iwana et al. [9] used triangular tabs attached at nozzle outlet and found that heat transfer can be improved through triangular tabs.

Swirling jets have high entrainment rates and are comprised of

* Corresponding author.
E-mail address: Naseem.uddin@utb.edu.bn (N. Uddin).

https://doi.org/10.1016/j.icheatmasstransfer.2018.12.002

Available online 02 January 2019

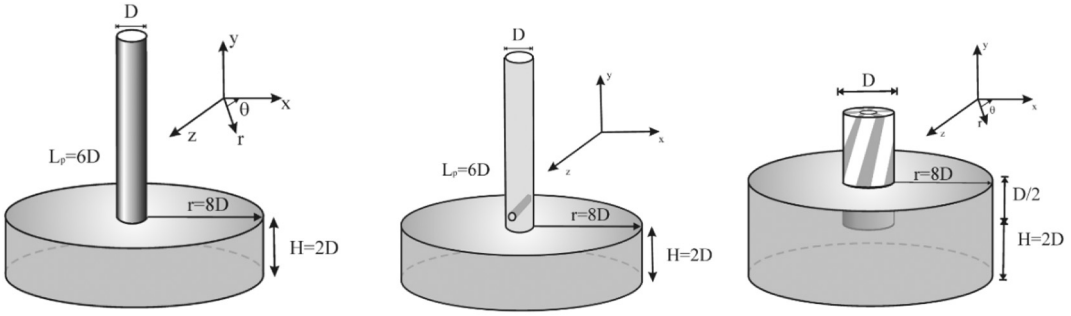

Fig. 1. Schematic diagram of the computational domains used for different simulations (a) non-swirling non excited jet, (b) passively excited jet with cylindrical insert, (c) swirling jet. A swirling device is shown for clarification but is not modelled.

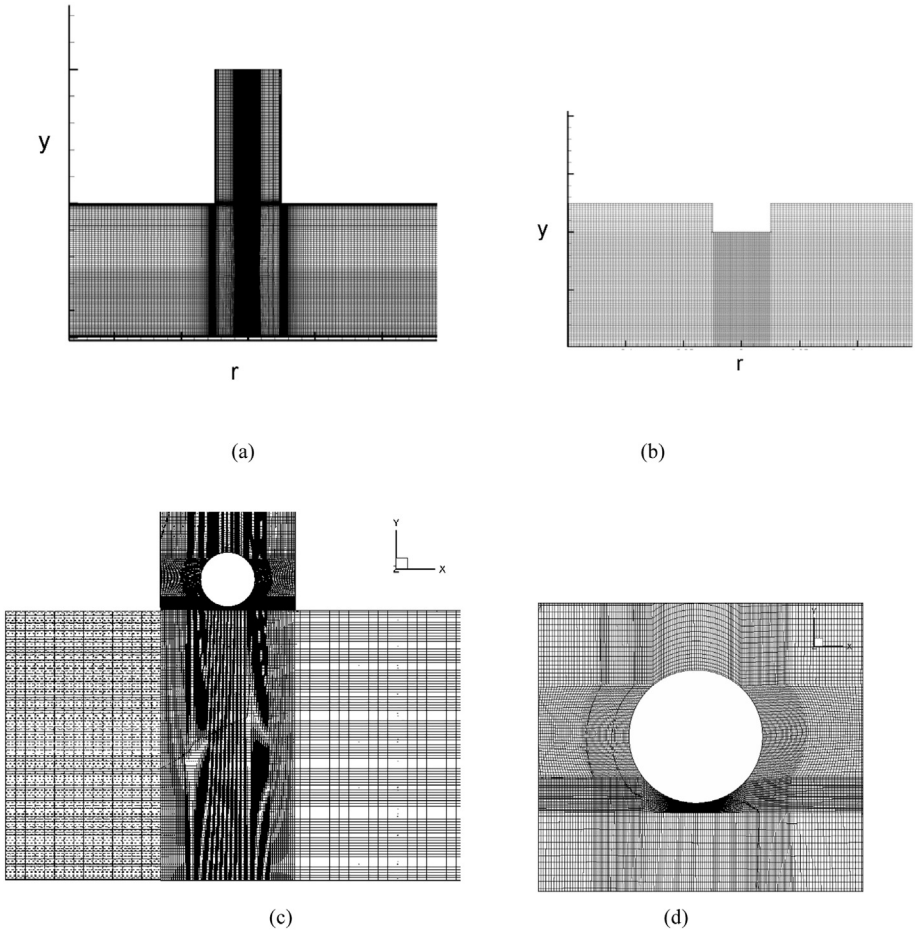

Fig. 2. Cross section of gird used for (a) natural and excited jet impingement (b) swirling jet impingement (c) jet impingement with cylindrical insert and (d) close-up view of grid around insert.

Table 1
Summary of cases studied and their corresponding grid size.

Case	Hexahedral grid size (millions)
Base flow	10
Swirling jet (S = 0.47)	6.4
Actively excited jet at harmonic frequency	10
Actively excited jet at sub-harmonic frequency	10
Passively excited jet with insert at jet's outlet	7.3

complex flow features like, spiral type flow instabilities, vortex break down and free shear layer. In the swirling jet the tangential velocity component plays an important role as it introduces additional instabilities in the jet. The swirl in the incompressible jet is quantified through a swirl number defined as the ratio of the angular to axial momentum fluxes [10]:

$$S = \frac{G_\theta}{RG_{ax}} = \frac{1}{R}\frac{\int_0^R r^2 u_{ax} u_\theta dr}{\int_0^R r u^2_{ax} dr} \quad (1)$$

where G_θ and G_{ax} are the tangential and axial momentum flux, u_θ and u_{ax} are the tangential and axial velocities of the swirling jet and R is the radius of the jet at outlet. A typical swirling flow normally has a core region behaving like a solid body rotation and a region away from the centre behaving more like a free vortex, the combination is known as Rankine vortex. Nozaki et al. [11] have proposed that there are two distinct modes of swirling jets, one is called heat transfer enhancement mode and other one the heat transfer suppression mode. The main role

Table 2
Grid details for different cases.

Cases	$\Delta r^+ = (\Delta r).u_\tau/\nu$	$r\Delta\theta^+ = (r\Delta\theta).u_\tau/\nu$	$\Delta_\perp{}^+$
Base flow	29	17	0.2
Swirling jet impingement	27	20	0.7
Jet with active excitation	29	17	0.2
Jet with passive excitation i.e. with insert	Impingement zone = 4 Wall jet zone = 16	Impingement zone =4 Wall jet zone = 94	0.5 near insert, 0.6 near impingement wall

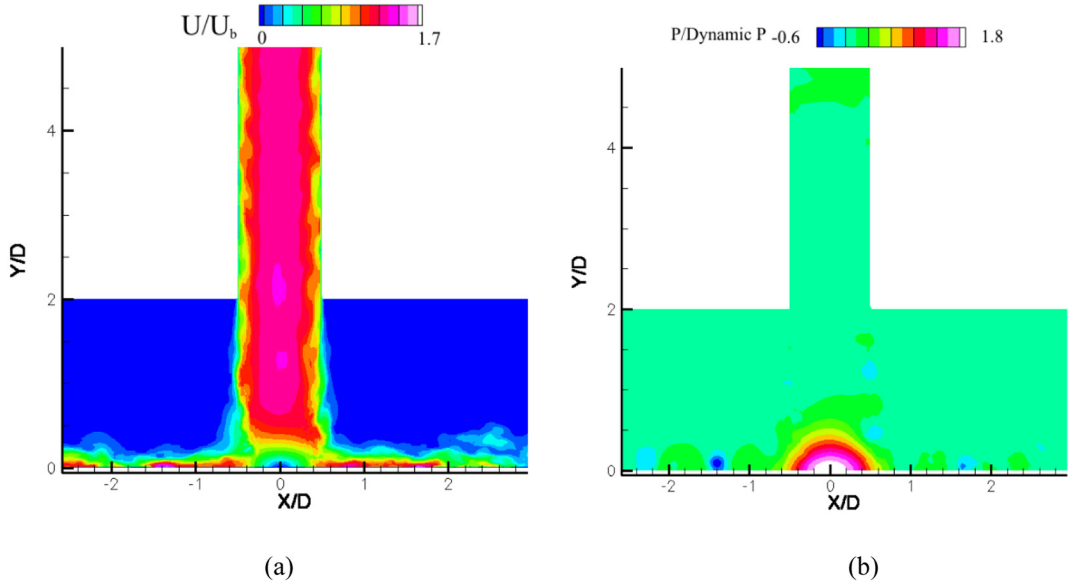

Fig. 3. (a) Instantaneous Velocity distribution in case of natural jet impingement (base flow) normalized by bulk inlet velocity (b) Instantaneous Pressure distribution in case of natural jet impingement (base flow) normalized by dynamic pressure.

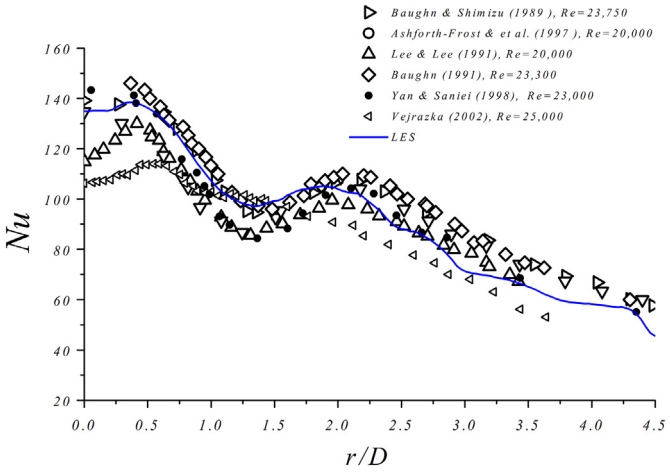

Fig. 4. Predicted and measured *Nu* for the 'base' flow.

is played by the dynamics of recirculation zones produced due to swirling jet impingement. The effects of swirl in impinging jet flow on heat transfer has been investigated experimentally by numerous researchers like [11–13]. This paper deals with the investigations related to a turbulent impinging jet. The goal is to assess the efficiency of swirl and excitations in enhancing the heat transfer at the target wall.

2. Mathematical formulation and computational details

In this study, the equations governing the conservation of mass, momentum and thermal energy were solved using finite-volume methodology with the effects of turbulence handled by adopting the Large-Eddy Simulations (LES) approach. The basis of this approach are well known and need not be reproduced here in detail. Briefly, the instantaneous equations are spatially averaged giving rise to variables that can be captured directly on the computational mesh, and to sub-grid scale correlations that must be approximated (see Pope [14]). The literature contains a number of different proposals for modelling the sub-grid scale correlations. Here, we adopt the dynamic model of Germano et al. [15] for the correlations in the filtered momentum equations, and a simple gradient-transport model for the correlations that appear in the thermal energy equation [16]. The thermal model involves the specification of a sub-grid Prandtl number which here was assigned the constant value of 0.9 [17,18].

Concerning the computations, these were performed using the FASTEST finite-volume solver [19] for three dimensional, time-dependent flows. The unsteady terms were discretised using the second-order accurate Crank-Nicholson scheme. The spatial gradients were discretised by central differencing which is also second-order accurate. The equations were solved implicitly with the value of Courant number kept constant at values < 1.0. The coupling between the continuity and momentum equations was achieved using the SIMPLE algorithm, and the system of coupled algebraic equations solved using Stone's Strongly-Implicit Procedure [19].

The solution domains for the three simulations performed are shown in Fig. 1. Also shown there relevant dimensions expressed as ratios of the jet exit diameter D. Representative computational grids are shown in Fig. 2. These were generated in block structured arrangements, and were concentrated in the regions where the greatest variations in flow parameters were expected to occur. The numbers of active meshes used for the cases considered are listed in Table 1. The grid spacing are listed in Table 2 where they are presented in wall co-ordinates. In specifying the boundary conditions, it was assumed that

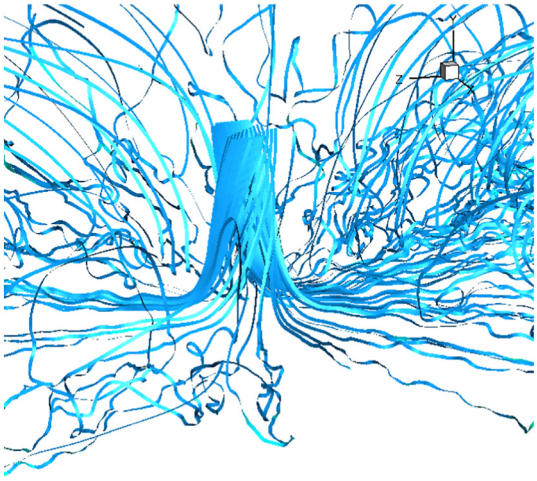

Fig. 5. Pathlines represented as ribbons and colored by temperature level for the flow in swirling jet impingement.

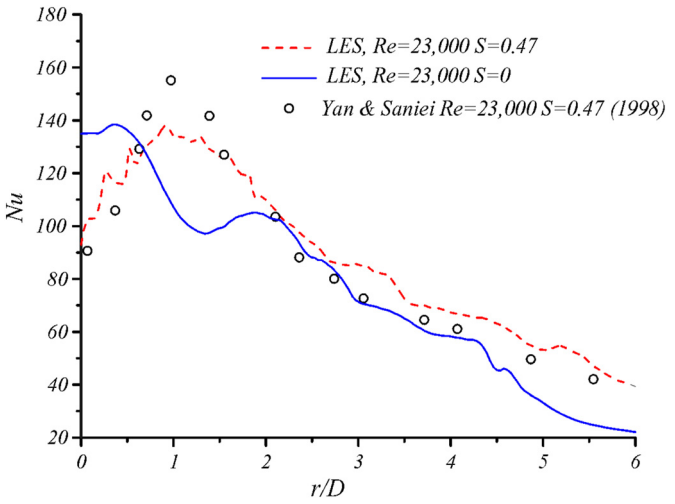

Fig. 6. Nusselt number distribution with and without swirl. Experimental data from ref. [26].

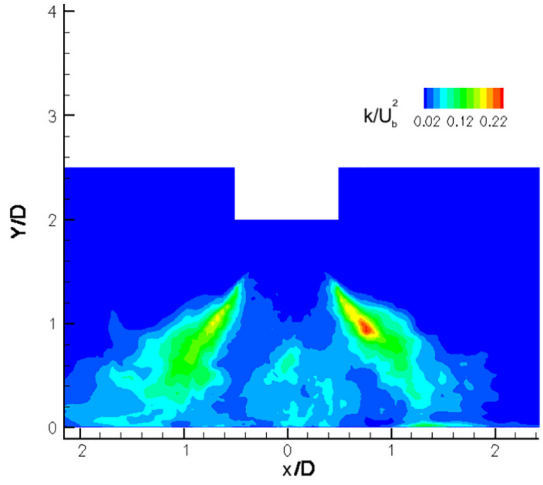

Fig. 7. Distribution of turbulent kinetic energy normalized by bulk inlet axial velocity.

the flow at exit from the pipe is fully developed and hence the velocity profile there was prescribed by combining the mean distribution of Kays et al. [20] with the digital-filter-based turbulence generation procedure proposed by Klein et al. [21].

For the case where active excitations of the jet's inlet flow field was considered, the jet's preferred mode was extracted from the energy spectrum of the velocity computed at various locations within the free region of the jet. The Strouhal number (based on the dominant frequency, the exit diameter and the bulk velocity) was found to be equal to 0.32. Once the dominant frequency of the free jet was thus determined, the jet's velocity was excited at half of its value (referred to as the subharmonic mode) and by twice of its value(referred as harmonic mode). This was achieved by perturbing the inlet flow velocity as:

$$U_{in} = U_b + A_N \sin(2\pi ft) \tag{2}$$

where U_{in} is the jet's inlet velocity and A_N is the amplitude of excitation which was here taken as 50% of the bulk inlet velocity (U_b).

For the swirling jet case, a tangential velocity was superimposed on the prescribed fully developed turbulent pipe flow. This was done using the proposal of Khalatov et al. [22]:

$$\frac{<u_\theta>}{u_\theta^*} = \left[\frac{2\vartheta}{1+\vartheta^2}\right]^{K^*} \tag{3}$$

where $\vartheta = r/r^*$, $r^* = 0.51R\phi_*^{0.41}$, $u_\theta^* = 2.04 < u_{ax} > \phi_*^{1.1}$

The quantity κ^* in Eq. (3) is an index depending on the swirl conditions and R is the radius at the jet's inlet. The parameter ϕ_* is comprised of swirl number and the axial momentum flux S/G_{ax}.

Concerning the thermal field, a constant temperature of 293 K was specified at the pipe exit. The heat flux at the target wall was set as 1000 W/m^2 in all simulations.

At outlets from the solution domain, a non-reflective boundary condition was applied as detailed in [16].

3. Results and discussion

3.1. The 'base' flow

To provide basis for assessing the various methods for heat-transfer enhancement, results were first obtained for the 'base' flow. The Reynolds number (based on jet diameter and bulk exit velocity) was set equal to 23,000 for which experimental data are available.

The Nusselt number is defined as:

$$Nu = \left(\frac{q_w''}{<T_W> - <T_j>}\right)\frac{D}{\lambda} \tag{4}$$

where, q_w'' is the heat flux $< Tw >$ is the temperature attained by the target wall after jet impingement and $< Tj >$ is the jet inlet temperature.

Fig. 3 (a) shows the contours of velocity distribution in the base flow in the domain. Velocity distribution is normalized by bulk velocity at the jet's inlet. Fig. 3 (b) shows pressure distribution inside jet normalized by dynamic pressure $\rho U_b^2/2$. As can be seen the pressure in the stagnation point is higher than surroundings. Also the cross-section of ring vortex can be seen indicated by low pressure zones.

Fig. 4 shows the radial distribution of the Nusselt number. The simulations were averaged in the azimuthal direction at target wall. Also plotted there are the experimental data of Baughn and Shimizu [23], Baughn et al. [24], Lee and Lee [25], Yan and Saniei [26], Ashforth-Frost et al. [27], Vejraska [28], Giovannini and Kim [29], Fenot [30]. The Reynolds number was slightly different in some of the measurements, varying in the range 20,000 - 23,300. The scatter in the measurements reflects the complex nature of this flow which transitions from being a free jet to a wall jet with significant entrainment of ambient fluid.

It has been found that the flow acceleration in the developing region of the wall jet is closely related to the secondary peak in the radial distribution of Nusselt number. In the thermally significant zone (lying in the range $1.4 < r/D < 2.8$) it is found that *hot* and *cold* spots

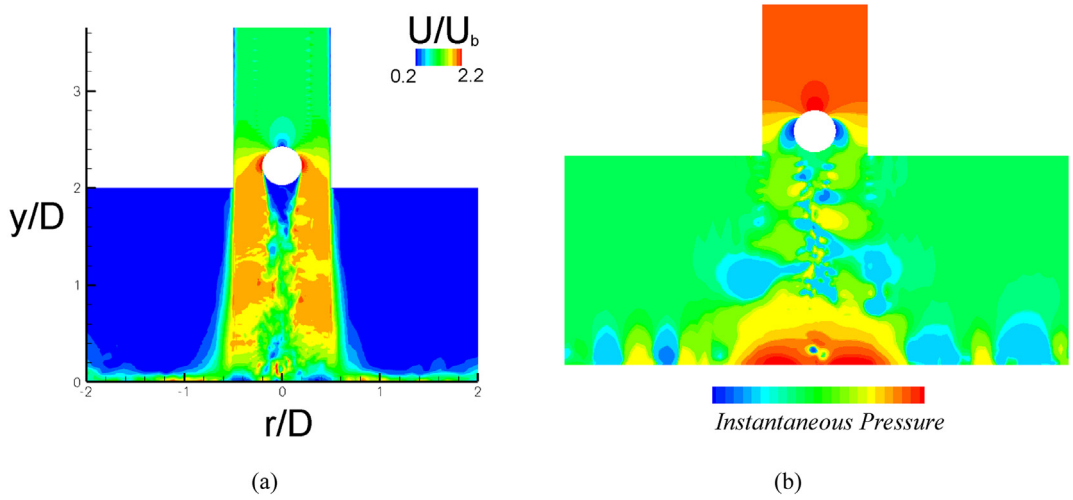

Fig. 8. (a) Flow over cylindrical insert and formation of twin jet system (a) Time averaged velocity distribution (b) Instantaneous pressure distribution.

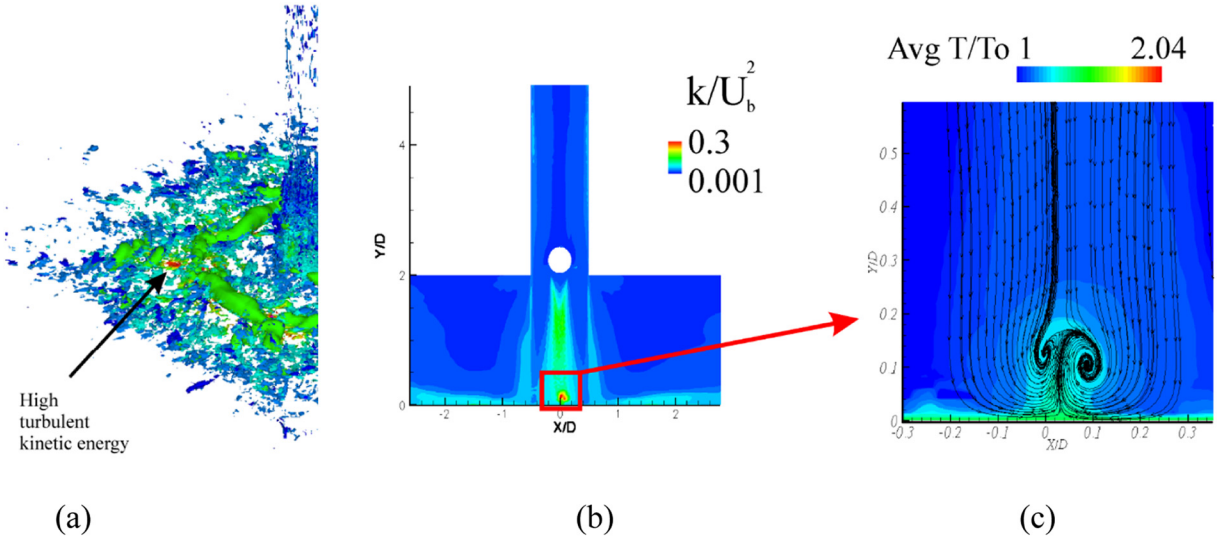

Fig. 9. Distribution of turbulent kinetic energy. (a) without insert (b) with insert (c) with insert near wall region.

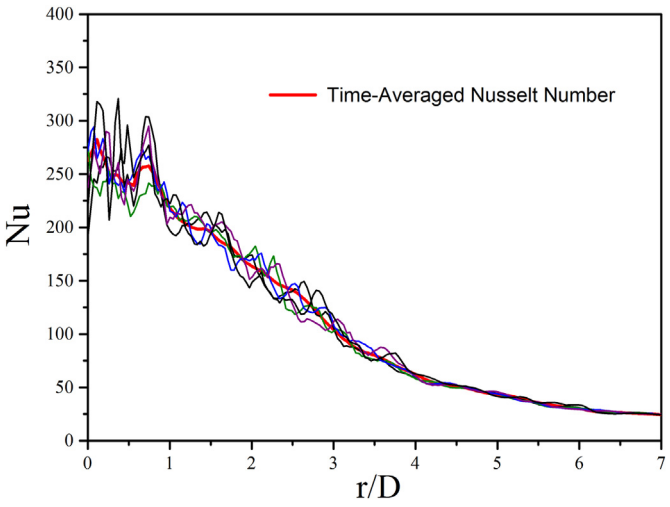

Fig. 10. Radial distribution of instantaneous Nusselt number at target wall.

appear side by side [7]. The second peak in the radial distribution of Nusselt number appear in this thermally significant zone. The peak in turbulent kinetic energy matches closely to the region where ring vortex is interacting with wall and broken-up into several pieces due to shear and elongation [7].

3.2. Enhancement with swirl

An overview of this flow can be seen from Fig. 5. Plotted there are the flow pathlines presented in the form of ribbons color coded according to the instantaneous temperature field. The twisted tape like appearance of jet stream shows that swirl has increased the shear and curvature effects of flow. Fig. 6 compares the Nusselt number distribution obtained with and without swirl being imparted to the inlet flow. The comparisons are with the experimental results of [24] which were obtained for swirl number S = 0.47. Senda et al. [12] have found that the location of the peak in the radial distribution of Nusselt number correlates strongly with the approaching maximum velocity near the wall. Also Abrantes and Azevedo [13] have found that turbulent kinetic energy can also be correlated with the peak in the radial distribution of the Nusselt number. Comparing Figs. 6 and 7 it can be inferred that in the case of a swirl number of 0.47, the peak in radial distribution of the Nusselt number is closely correlated with the occurrence of the

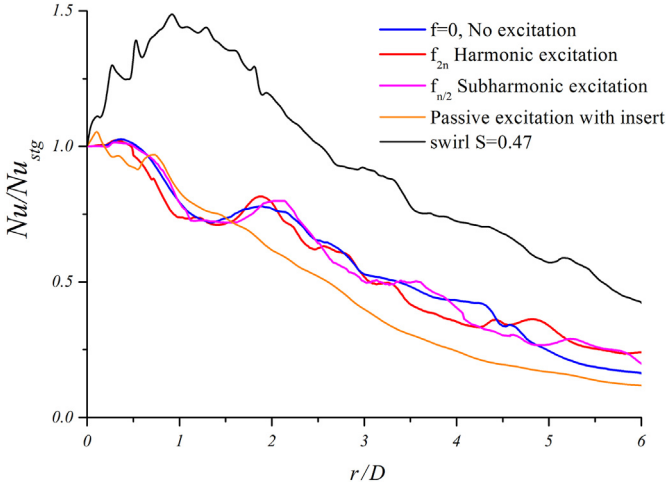

Fig. 11. Time averaged normalized *Nu* distribution.

maximum turbulent kinetic energy close to the wall.

3.3. Enhancement with passive excitations

The passive excitations were generated by placing a cylindrical insert inside the pipe and by computing the flow around it. The insert, which was of diameter ratio d/D = 0.5, was placed just before the jet exit (see Fig. 1(b), Fig. 2 (c) or Fig. 2 (d)). It was expected that vortex shedding will occur since the resulting Reynolds number (based on insert diameter) was 11, 500.

Time-averaged contours of mean velocity and instantaneous static pressure are shown in Fig. 6. Fig. 6 (b) shows the instantaneous pressure in jet. As can be seen at stagnation region two distinct high pressure impingement zones are formed. This cause more intense mixing of the flow in this region which significantly affect the turbulent kinetic energy as can be seen in Fig. 8. Fig. 8 (a) shows the distribution of turbulent kinetic energy in base flow. Fig. 8 (b) and (c) show the distribution of turbulent kinetic energy in insert assisted passive excitations case. As can be noticed the kinetic energy is very high in the stagnation zone of the jet. Compared to the no-insert case, there is a 30% increase in the turbulent kinetic energy in the domain. Figure shows the close up view of the stagnation zone. Here the time averaged pathlines are plotted. The contour shows the time averaged temperature field, which is normalized by the jet's inlet temperature value. The target wall is heated with a constant heat-flux, therefore the flow there is hot. The flow coming from the cylindrical insert, sweeps the geometrical stagnation zone and an up-wash region is created. This complex flow dynamics has tremendous effects on the heat transfer distribution. It is found that under this highly complex flow field the heat transfer at the target wall is strongly enhanced. Fig. 9 shows the instantaneous Nusselt number distribution at the target wall. The red bold line shows the time averaged Nusselt number. After r/D > 4, the influence of these fluctuations is no longer detectable.

3.4. Enhancement with active excitations

Fig. 10 shows instantaneous Nusselt number distribution for jet impingement with insert case whereas Fig. 11 shows normalized Nusselt number distribution for all four cases. The inclusion of insert would definitely enhance the heat transfer compared to other cases discussed in this paper. Moreover placing an insert in flow is more simplistic procedure than controlling the swirling device and pulsing of jet. The inclusion of cylindrical insert in impinging jet would lead to pressure loss.

$$\frac{P_1 - P_2}{\frac{1}{2}\rho U_b^2} \approx 3 \tag{5}$$

where P_1 and P_2 are time-averaged pressures before and after insert. However pressure loss would also occur due to swirling device and pulsating mechanism installed. Therefore a conclusive statement on pressure loss cannot be made.

4. Conclusions

It is found that:

- In case of active jet velocity field excitations, the choice of active excitation frequency plays an important role in terms of enhancement of heat transfer. Also enhancement in heat transfer is higher for a harmonic excitation compared with the subharmonic excitation of the preferred mode. For an appreciable enhancement to be achieved, the amplitude of excitations should also be high (taken 50% of jet's bulk velocity here). See Eq. (2).
- In case of a swirling jet, the swirl for the investigated swirl number did not lead to an appreciable enhancement in heat transfer.
- The passive excitations of jet by introducing an insert in the jet nozzle causes improved heat transfer which is much higher than that achieved by active excitation and swirl.

Acknowledgments

The authors would like to thank Prof. Dr. M. Schäfer and Dr.-Ing. D. Sternel, Fachgebiet für Numerische Berechnungsverfahren im Maschinenbau (FNB), Technische Universität, Darmstadt, Germany for providing the FASTEST code and helpful discussions.

References

[1] E. Gutmark, C. Ho, Preferred modes and the spreading rates of jets, Phys. Fluids 26 (10) (1983) 2932–2938.
[2] C. Gau, W.Y. Sheu, C.H. Shen, Impingement cooling flow and heat transfer under acoustic excitations, J. Heat Transf. 119 (1997) 810–817.
[3] S.D. Hwang, H.H. Cho, Effects of acoustic excitation positions on heat transfer and flow in axisymmetric impinging jet: main jet excitation and shear layer excitation, Int. J. Heat Fluid Flow 24 (2003) 199–209.
[4] H.S. Sheriff, D.A. Zumbrunnen, Effect of flow pulsation on cooling effectiveness of an impinging jet, J. Heat Transf. 116 (1994) 886–895.
[5] Z. Travnicek, L. Nemcova, J. Kordik, V. Tesar, V. Kopecky, Axisymmetric impinging jet excited by a synthetic jet system, Int. J. Heat Mass Transf. 55 (2012) 1279–1290.
[6] P. Jiang, Y.C. Guo, C.K. Chan, W.Y. Lin, Frequency characteristics of coherent structures and their excitations in small aspect-ratio rectangular jets using large eddy simulation, Comput. Fluids 36 (2007) 611–621.
[7] N. Uddin, S.O. Neumann, B. Weigand, Heat transfer enhancement by velocity field excitation for an impinging round jet, J. Numer. Heat Transf. A 69 (2016) 811–824.
[8] H. Herwig, H. Mocikat, S. Göppert Gürtler, Heat transfer due to unsteadily impinging jets, Int. J. of Thermal Sci. 43 (2004) 733–741.
[9] T. Iwana, K. Suenaga, K. Shirai, Y. Kameya, M. Motosuke, S. Honami, Heat transfer and fluid flow characteristics of impinging jet using combined device with triangular tabs and synthetic jets, Exp. Thermal Fluid Sci. 68 (2015) 322–329.
[10] A.K. Gupta, D.G. Lilley, N. Syred, Swirl Flows, Gordon & Breach Science Publishers, 1984.
[11] A. Nozaki, Y. Igarashi, K. Hishida, Heat transfer mechanism of a swirling impinging jet in a stagnation region, Heat Transf. Asian Res. 32 (8) (2003) 663–673.
[12] M. Senda, K. Inaoka, D. Toyoda, S. Sato, Heat transfer and fluid flow characteristics in a swirling impinging jet, Heat Transfer Asian Research 34 (5) (2005) 324–335.
[13] J.K. Abrantes, L.F.A. Azevedo, Fluid flow and heat transfer characteristics of a swirl jet impinging on a flat plate, Annals Assembly for Int. Heat Transfer Conference, 2006.
[14] S.B. Pope, Turbulent Flows, Cambridge University Press, United Kingdom, 2000.
[15] M. Germano, U. Piomelli, P. Moin, W.H. Cabot, A Dynamic Subgrid-Scale Eddy Viscosity Model, Phys. Fluids A 3 (7) (1991) 1760–1765.
[16] D. Sternel, FASTEST, User Manual, Department of Numerical Methods in Mechanical Engineering, Technische Universität Darmstadt, 2005.
[17] M. Breuer, Direkte Numerische Simulation Und Large-Eddy Simulation Turbulenter Strömungen Auf Höchleistungrechnern, Habilitation Thesis, Shaker Verlag, 2002.
[18] N. Uddin, Turbulence Modeling of Complex Flows in CFD, PhD Thesis, Universitaet Stuttgart, Germany, 2008.
[19] H.L. Stone, Iterative solution of implicit approximations of multidimensional partial differential equations, SIAM J. Numer. Anal. 5 (1988) 530–558.
[20] W.M. Kays, M.E. Crawford, B. Weigand, Convective Heat and Mass Transfer,

McGraw-Hill, USA, 2004.
[21] M. Klein, A. Sadiki, J. Janicka, A digital filter based generation of inflow data for spatially direct numerical or large Eddy simulations, J. Comput. Phys. 18 (2003) 652–665.
[22] A.A. Khalatov, A.A. Avramenko, I.V. Shevchuk, Heat transfer and fluid flow in the fields of centrifugal forces, Swirl flows, Vol-III, Russian edition, National Academy of Sciences of Ukraine, Institute of Engineering Thermophysics, Kiev, 2002.
[23] J.W. Baughn, S. Shimizu, Heat transfer measurement from a surface with uniform heat flux, and an impinging jet, Int. J. Heat Transf. 111 (1989) 1096–1098.
[24] W.J. Baughn, A.E. Hechanova, X. Yan, An experimental study of entrainment effects on the heat transfer from a at surface to a heated circular impinging jet, J. Heat Transf. 113 (1991) 1023–1025.
[25] J. Lee, S. Lee, Stagnation region heat transfer of a turbulent axisymmetric Jet impingement, Exp. Heat Transfer 12 (1999) 137–156.
[26] X. Yan, N. Saniei, Heat Transfer Measurements From a Flat Plate to a Swirling Impinging Jets, Pro. 11th Int. Heat Transfer Conference, Kyonju, Korea, 1998.
[27] S. Ashforth-Frost, K. Jambunathan, C.F. Whitney, S.J. Ball, Heat transfer from a flat plate to a turbulent axisymmetric impinging jet, Proc. Instn. Mech. Engrs. 211 (Part C) (1997) 167–172.
[28] J. Vejrazka, Experimental Study of Pulsating Round Impinging Jet, PhD Thesis, 2002 Institute of Chemical Process Fundamentals, Prague, 2002.
[29] N.S. Kim Giovannini, Impinging jet: Experimental analysis of fluid field and heat transfer for assesment of turbulent models, Annals of the Assembly for Int. Heat Transfer Conference, 13 2006 (TRB-15, 2006).
[30] M. Fenot, Etude du refroidissement par impact de jets. application aux aubes de turbines, PhD Dissertation, 2004 Université de Poitiers, France, 2004.